Similarly the second term is singular when $\mathbf{s}'\|(\mathbf{s}-\mathbf{s}')$ and

$$1-\omega^2/(v_F s')^2=0. \tag{A19}$$

(2) $L<0$. Inspection of I_{1p} when $L<0$ shows that again the first term is singular when $1-\omega^2/(v_F s)^2=0$, and the second term when $1-\omega^2/(v_F s')^2=0$.

Finally we note that I_{1p} is an even function of ω and therefore will only contribute to the $\zeta(2)$ terms of $R(z)$.

B. The δ Function

$$I_\delta=\frac{i\pi}{2}\int_{-1}^{1}\frac{\partial}{\partial\omega}\delta(\Gamma_Q-\omega)d\nu,$$

i.e.,

$$I_\delta=-\frac{i\pi}{2V_F|\mathbf{Q}|}\int_0^1[\delta(v_F|\mathbf{Q}|-\omega)-\delta(v_F|\mathbf{Q}|+\omega)]du. \tag{A20}$$

We see by inspection that I_δ is an odd function of ω and therefore will contribute only to the $\zeta(3)$ terms of $R(z)$. We may also easily check that $I_\delta(\mathbf{q},\mathbf{q})$, the only term arising in the power absorption, is identically zero.

PHYSICAL REVIEW VOLUME 148, NUMBER 1 5 AUGUST 1966

Mössbauer Hyperfine Spectra of Fe^{3+} in Corundum: Magnetic- and Crystal-Field Effects

H. H. WICKMAN AND G. K. WERTHEIM
Bell Telephone Laboratories, Murray Hill, New Jersey
(Received 16 February 1966)

The Mössbauer technique was employed to study the paramagnetic hfs of Fe^{57}-doped corundum (α-Al_2O_3) in the presence of an external magnetic field. Experiments were performed with an oriented single crystal and with external field strengths to 41 kOe parallel to the trigonal axis of the crystal field at the iron site. The results showed noticeable field-dependent features. Several of these effects were analyzed by detailed calculations of theoretical hfs from the ground-term electronic levels of Fe^{3+}. Effects of small local fields and of mixing of electronic states by crystal-field terms and by the hyperfine interaction are shown to produce gross changes in the Mössbauer spectra. Some of these features were observed; others which require a more homogeneous magnetic field were not observed because major changes in the Mössbauer spectra occur over relatively small ranges of external field strengths.

I. INTRODUCTION

IN previous work, the well-resolved, low-temperature paramagnetic hyperfine spectra of trivalent Fe^{57} in corundum (Al_2O_3) have been investigated by Mössbauer effect, primarily in the absence of an external magnetic field.[1–3] The major features of the Mössbauer absorption spectrum in zero field were explained on the basis of the "superposition" of three essentially independent hfs from the three Kramers doublets of the ground term of Fe^{3+}: $3d^5$, $^6S_{5/2}$. However, the observed and predicted spectra for the ground doublet were not in complete agreement. Since the spin-Hamiltonian parameters of Fe^{3+} in Al_2O_3 are known to high accuracy[4–6] so that theoretical hfs are readily calculated, we have extended these measurements to study magnetic-field-dependent features of the hfs and to obtain further comparisons of experiment with theory.

It is known from ESR work that a relatively small cubic term in the spin Hamiltonian causes a large mixing of electronic wave functions for certain critical-field strengths. It is shown below that this leads to dramatic changes in the hfs for small changes of the externally applied magnetic field. The magnetic field also causes certain levels to cross. At these points equally

[1] G. K. Wertheim and J. P. Remeika, Phys. Letters **10**, 14 (1964).

[2] G. K. Wertheim and J. P. Remeika, in *Proceedings of the XIII Colloque Ampere, Louvain, Belgium, 1964* (North-Holland Publishing Company, Amsterdam, 1965), pp. 147–161.

[3] C. E. Johnson, T. E. Cranshaw, and M. S. Ridout, in *Proceedings of the International Conference on Magnetism, Nottingham, 1964* (The Institute of Physics and the Physical Society, London 1964), pp. 459–461.

[4] L. S. Kornienko and A. M. Prokhorov, Zh. Eksperim. i Teor. Fiz. **36**, 919 (1959); **40**, 1594 (1961) [English transls.: Soviet Phys.—JETP **9**, 649 (1959); **13**, 1120 (1961)].

[5] H. F. Symmons and G. S. Bogle, Proc. Phys. Soc. (London) **79**, 468 (1962).

[6] J. H. Pace, D. F. Sampson, and J. S. Thorp, Proc. Phys. Soc. (London) **78**, 257 (1961).

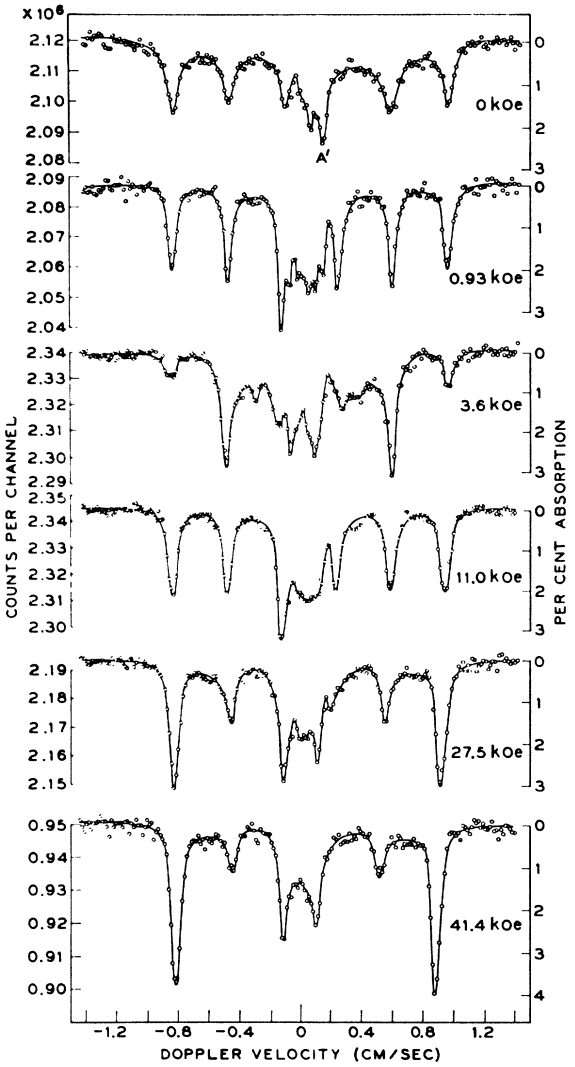

FIG. 1. Paramagnetic hyperfine structure of Fe^{57}-doped Al_2O_3. The external magnetic field strengths are indicated; the absorber temperature was 4.2°K. *Note added in proof.* The Mössbauer lines at high field are significantly shifted from their theoretical positions because the Co^{57} in copper source was in the fringing field of the superconducting solenoid. Consideration of the resulting nuclear Zeeman effect in the source and of the polarization of both source and absorber transitions shows that this increases the separation of the outer line and decreases that of the inner lines. This effect is negligible at fields below 10 kOe.

large changes in the hfs occur as a result of the mixing of states by the hyperfine interaction. Since such behavior should be typical of other paramagnetic iron systems detailed theoretical spectra are given.

It is also shown that in the limit of small applied field, where the Zeeman interaction is of the order of the hyperfine interaction, the hfs of the ground doublet is greatly modified. The zero-field case is never obtained experimentally because of local dipolar fields from neighboring nuclei. Such fields, which are of the order of 10 Oe. are sufficient to distort the zero-field "static hyperfine pattern" calculated for the ground doublet, $\sim|\pm\frac{1}{2}\rangle$. These considerations together with the complication of enhanced relaxation in this doublet[1,2] suggest that observation of the static hfs in this type of system will in general be difficult.

II. EXPERIMENTAL

The measurements employed a conventional linear velocity-sweep drive system[7] and a Westinghouse NbZr superconducting solenoid. The oriented, single-crystal Fe^{57}-doped corundum absorber was the same one used in the previous experiment.[1,2] It was grown from PbO $(B_2O_3)_x$ flux at conditions where the growth habit favors flat c-axis plates; i.e., the trigonal axis of the iron site is perpendicular to the plane of the plate. This is convenient for our experiments in that the magnetic field direction was desired parallel to the trigonal axis to avoid the immediate mixing of crystal-field states by the applied field. In addition the use of γ rays propagating parallel to the trigonal axis implies that $\Delta m=0$ transitions have zero intensity. The relative intensities for an effective hyperfine field spectrum under these conditions are 3:0:1:1:0:3.

The data obtained at 4.2°K for field strengths between 0 and 42 kOe are shown in Fig. 1. Since the absorber contained only 0.1 mg/cm² of Fe^{57}, the accumulation of statistically significant data required counting periods of up to 36 h. Results obtained with more concentrated absorbers have been previously reported,[2] but the hfs spectra are then broadened by spin-spin interactions making interpretation much more difficult. The concentration of Fe^{57} employed here was about 10^3 times greater than that commonly used in ESR experiments. However, the sample used in the Mössbauer work was also checked with ESR and gave a reasonance spectrum in agreement with that reported by previous workers.[4–6]

The resolution of the Mössbauer spectra was limited in some cases by the homogeniety of the magnetic field. A nonuniformity of 5% over the sample volume was estimated from the specifications of the solenoid. This is sufficient to preclude observation of the details of certain paramagnetic hfs discussed below. However, other field-dependent effects are immediately apparent. Between 0 and 0.93 kOe a significant change in the inner structure of the spectrum occurred, and the relative intensities of the four outer lines reversed. At 0.93 kOe the noticeable unresolved background "smear" seen in the zero-field data is essentially absent. At a field of 3.6 kOe a drop in intensity of the two outer lines is accompanied by an increase in intensity of the next pair of lines, together with the appearance of unresolved resonances interior to the latter pair of lines.

[7] R. L. Cohen, P. G. McMullin, and G. K. Wertheim, Rev. Sci. Instr. 34, 671 (1963).

III. CRYSTAL-FIELD THEORY

When trivalent iron substitutionally replaces Al^{3+} in corundum, the ground term of the $3d^5$ configuration is ^6S which is characteristically only weakly perturbed by the crystal field. There are two inequivalent sites for iron. For a particular site, the electronic-spin Hamiltonian, from ESR work, is

$$\begin{aligned}\mathcal{H}\equiv\mathcal{H}_z+\mathcal{H}_{cf}=g\beta\mathbf{H}\cdot\mathbf{S}+D[S_z^2-(\tfrac{1}{3})S(S+1)]\\ +(a/6)[S_\xi^4+S_\eta^4+S_\zeta^4-(\tfrac{1}{5})S(S+1)(3S^2+3S-1)]\\ +(F/180)[35S_z^4-30S(S+1)S_z^2+25S_z^2\\ -6S(S+1)+3S^2(S+1)^2],\end{aligned}\quad(1)$$

where g is the spectroscopic splitting factor, assumed isotropic with spin-only value 2.0; $S=\frac{5}{2}$; and the other terms have their usual meanings. For each site there is a coordinate system (ξ,η,ζ) which lies along the cubic axes of the crystal field while the z axis of $\mathcal{H}$ is directed along the cubic axes of the crystal field while the z axis of $\mathcal{H}$ is directed along the [111] axis of (ξ,η,ζ). Fortunately, the two sites differ simply in the relative orientation of their cubic axes and one system may be derived from the other by a rotation of 60° about the z axis of $\mathcal{H}$. In our experiments the external field is applied along the z direction in (1) so that both sites are magnetically equivalent for our purposes. Thus, only one site need be considered and the relative orientation of the (x,y) axes and the (ξ,η,ζ) system is immaterial. This is useful because a proper choice of this orientation allows $\mathcal{H}$ to be represented by a real 6×6 matrix, which considerably simplifies the calculation discussed below.

In addition to $\mathcal{H}_{cf}$, there are the hyperfine interaction, $\mathcal{H}_{hf}$, and quadrupole interaction, $\mathcal{H}_q$. For Fe^{3+} the contact hyperfine term arising from core polarization is dominant and

$$\mathcal{H}_{hf}=A\mathbf{I}\cdot\mathbf{S},\quad(2)$$

where the value of A has been recently accurately determined by ENDOR techniques.[8] Because of the trigonal symmetry of the crystal field the appropriate quadrupole interaction is directed in the z direction and is, in the conventional form,

$$\begin{aligned}\mathcal{H}_q=(e^2qQ/4I(2I-1))[3I_z^2-I(I+1)]\\ \equiv P[I_z^2-(\tfrac{1}{3})I(I+1)],\end{aligned}\quad(3)$$

where $I=\frac{3}{2}$ for the excited state of Fe^{57} and P is determined experimentally.

In the Mössbauer effect, transitions are induced between states of the Hamiltonian for the ground-state hyperfine levels,

$$\mathcal{H}_g=\mathcal{H}_g(S,I_g)=\mathcal{H}_z(S)+\mathcal{H}_{cf}(S)+\mathcal{H}_{hf}(S,I_g)\quad(4)$$

and levels of the excited state given by the Hamiltonian

$$\mathcal{H}_e=\mathcal{H}_z(S)+\mathcal{H}_{cf}(S)+\mathcal{H}_{hf}(S,I_e)+\mathcal{H}_q(I_e).\quad(5)$$

The dimension of the matrix representing H_g is $(2S+1)(2I_g+1)=12$, and the matrix of $\mathcal{H}_e$ is $(2S+1)(2I_e+1)=24$ dimensional. The values of the parameters introduced to this point were taken as[5,8]

$$\begin{aligned}D&=0.1719\text{ cm}^{-1}=44.39\text{ cm/sec},\\ a&=0.0229\text{ cm}^{-1}=5.93\text{ cm/sec},\\ F&=-0.0112\text{ cm}^{-1}=-2.89\text{ cm/sec},\\ A_e&=+0.149\text{ cm/sec},\\ A_g&=-0.261\text{ cm/sec},\\ P&=+0.025\text{ cm/sec}.\end{aligned}\quad(6)$$

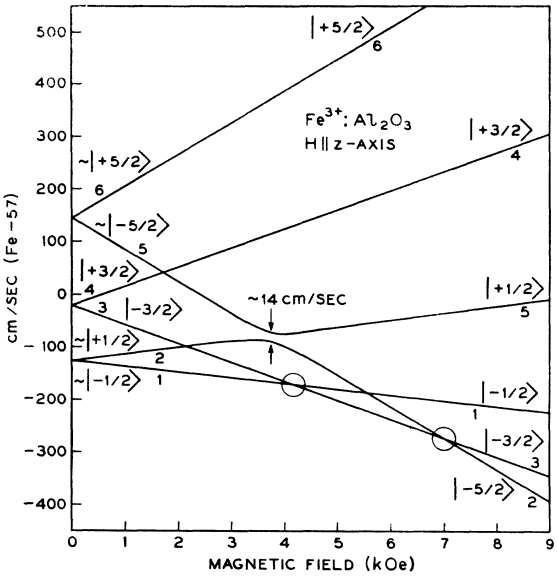

FIG. 2. Crystal-field levels for Fe^{3+} in Al_2O_3 with $H\|z$ axis, for the field strengths indicated.

So far we have neglected the direct interaction of the nuclear moments with an external field. This interaction is small but is included for completeness in the Hamiltonians. For the excited and ground states, we have

$$\mathcal{H}_{em}=\mu_{ez}H_z=g_e\beta_N H_z I_{ez},\quad(7)$$

and

$$\mathcal{H}_{gm}=\mu_{gz}H_z=g_g\beta_N H_z I_{gz},\quad(8)$$

to be added to $\mathcal{H}_e$ and $\mathcal{H}_g$, respectively.

Before discussing γ-ray transitions, it is instructive to set $A=P=g_e=g_g=0$ and consider only the effect of the external field on the crystal-field levels of $\mathcal{H}_g$ (or $\mathcal{H}_e$), i.e., we look at $\mathcal{H}=\mathcal{H}_z+\mathcal{H}_{cf}$. Figure 2 shows the levels for low fields and Fig. 3 gives the level diagram extended to high fields where M_S becomes a good quantum number. The level crossings or repulsions in Fig. 2 are of primary concern. At approximately 3.7 kOe, for example, the small cubic "a" term is responsible for a large mixing of two of the crystal-field levels. The two states which repel each other here have nearly equal admixture of the $|M_S=-\frac{5}{2}\rangle$ and $|M_S=\frac{1}{2}\rangle$ states. Denoting them by Ψ_2 and Ψ_5, they are $\Psi_2\cong(1/\sqrt{2})(|\frac{1}{2}\rangle+|-\frac{5}{2}\rangle)$ and $\Psi_5\cong(1/\sqrt{2})(|\frac{1}{2}\rangle-|-\frac{5}{2}\rangle)$ and we see

[8] P. R. Locher and S. Geschwind, Phys. Rev. 139, A991 (1965).

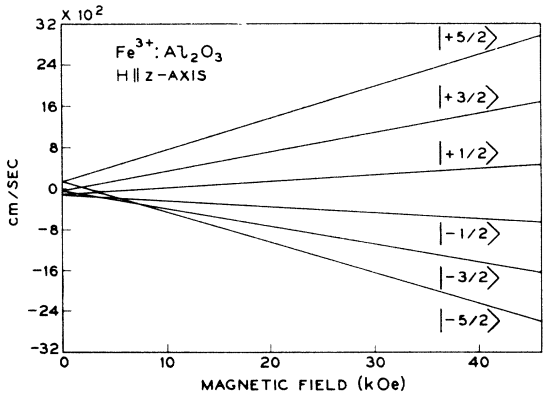

FIG. 3. Electronic levels of Fe^{3+} in Al_2O_3 extended to Zeeman region of high field strengths.

$\langle\Psi_i|S_z|\Psi_i\rangle=-1$, $i=2$, 5. That is, $\langle\Psi_2|S_z|\Psi_2\rangle$ changes from $\frac{1}{2}$ to $-\frac{5}{2}$ as H goes from 3 to 4 kOe; similarly $\langle\Psi_5|S_z|\Psi_5\rangle$ changes from $-\frac{5}{2}$ to $\frac{1}{2}$. These changes will, of course, markedly affect the hyperfine splittings which, in this case, are proportional to $A\langle S_z\rangle$. This is illustrated by calculated spectra below.

Other level crossings such as at $H=4.3$ and 6.9 kOe are important because here the addition of the hyperfine interaction will mix wave functions [through terms like $(A/2)I_+S_-$] and destroy the effective-field approximation mentioned above. These effects are best illustrated by theoretical spectra.

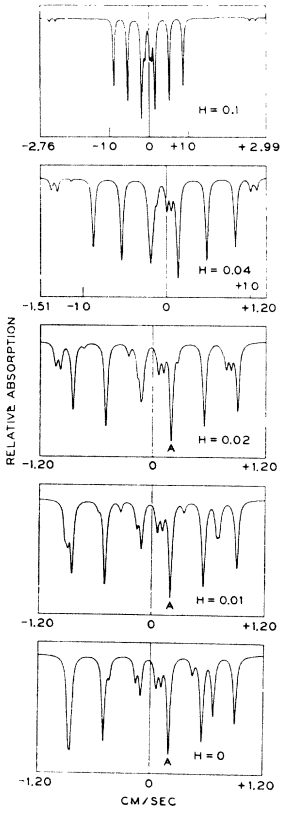

FIG. 4. Paramagnetic hyperfine spectra calculated from spin-Hamiltonian parameters, and small external magnetic field.

The calculation of such spectra requires a few additional facts. We note that the source γ ray beam is parallel to the nuclear quantization axis, so that $\Delta m_I=0$ transitions have vanishing intensity. A further selection rule of considerable importance is that of $\Delta M_S=0$ during the nuclear transitions. This follows simply because we are in the direct-product representation, $|M_S\rangle|m_I\rangle$, and the $M1$ nuclear operator does not connect different electronic substates. Since our experiments were performed at 4.2°K, it was also necessary to include a Boltzmann factor for the population of the ground-state hyperfine levels. Finally, a quadrupole interaction P, of +0.025 cm/sec as deduced from experiment,[1,2] was included in the calculation. The details of the calculations are straightforward and are given in the Appendix.

Several sets of representative spectra are shown in Figs. 4–7. They can be interpreted in terms of a Breit-Rabi treatment for the electron-nuclear system. It is useful to discuss separately three regions of magnetic field: (1) $0\leq H\leq 1$ kOe; (2) $3.0\leq H\leq 4.0$ kOe; and (3) $4.2\leq H\leq 4.4$ and $6.8\leq H\leq 7.9$ kOe.

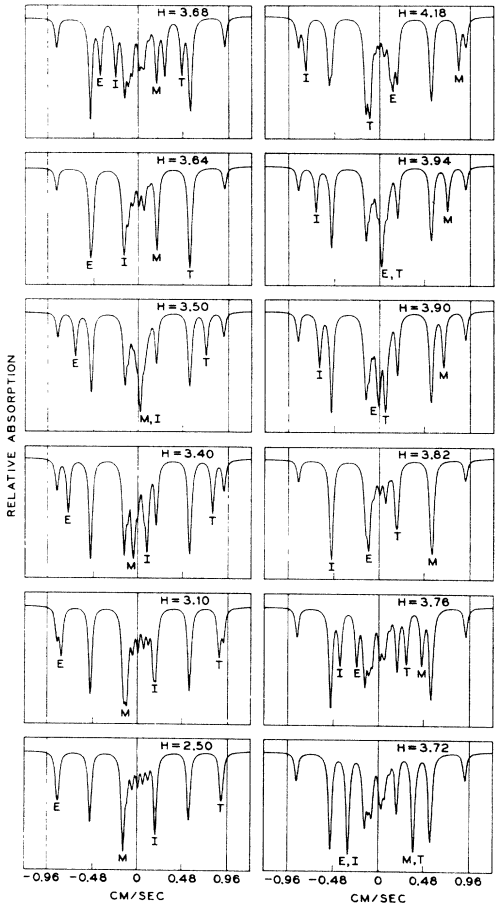

FIG. 5. Hyperfine spectra in the presence of mixing of states by a crystal-field term.

(1) For $H=0$, a superposition of the hfs from the three Kramers doublets of composition $|\pm\frac{5}{2}\rangle$, $|\pm\frac{3}{2}\rangle$, and $|\pm\frac{1}{2}\rangle$ are observed. In the $|\pm\frac{5}{2}\rangle$ and $|\pm\frac{3}{2}\rangle$ levels the hyperfine interaction cannot mix the crystal-field states; M_S and m_I are good quantum numbers, and the effective-field approximation is valid (the $|M_S\rangle|m_I\rangle$ are eigenstates). Each of these two doublets gives rise to four hyperfine lines with relative intensities 3:0:1:1:0:3, and with spacings corresponding to fields of ± 550 and ± 330 kOe for the $|\pm\frac{5}{2}\rangle$ and $|\pm\frac{3}{2}\rangle$ levels, respectively. As shown in previous work, the effective fields are given by $H_{\text{eff}}=220\langle S_z\rangle$ kOe.

The $|\pm\frac{1}{2}\rangle$ doublet in zero field is more complicated due to the hyperfine interaction which in this case greatly admixes the $|M_S\rangle|m_I\rangle$ basis states. Here seven lines with relative intensities (1.75:0.5:3.0:0.05:0.25:0.5:1.95) are predicted. The latter spectrum is not in complete agreement with the experimental data; however, a consideration of this is postponed until the discussion.

As a small field (5–10 Oe) is applied, (Fig. 4) the electronic Zeeman interaction is of the order of 0.1 cm/sec and certain of the lines from the lower Kramers doublet hfs begin to move rapidly as a function of field strength. They are simply a measure of the admixture of, say, $|+\frac{1}{2}\rangle|m_{Ie}\rangle$ into a state composed largely of $|-\frac{1}{2}\rangle m_{Ie}+1\rangle$; this allows transitions from a ground hyperfine state containing $|+\frac{1}{2}\rangle|m_{Ig}=m_{Ie}\pm 1\rangle$. These effects continue so long as the interaction of the ion with the field is small and is due to the electronic Zeeman energy which for fields of 10 Oe is of the same order as

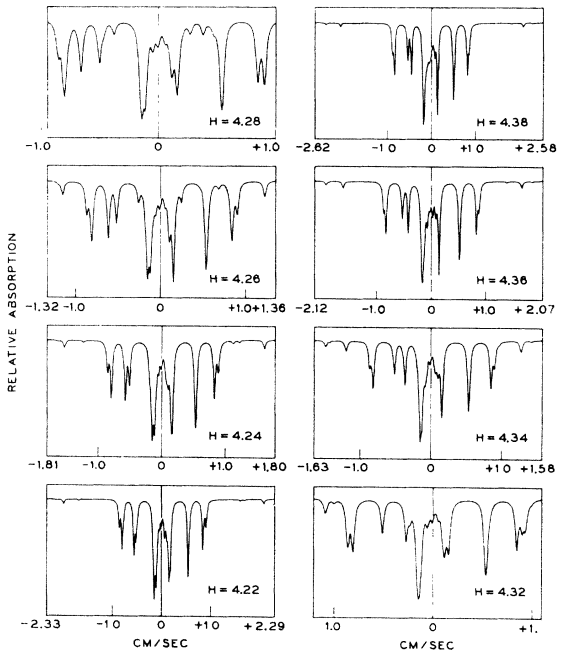

FIG. 6. Hyperfine spectra in the presence of mixing of states by the hyperfine interaction ($H\cong 4.3$ kOe). Markers have been placed at ± 1.0 cm/sec.

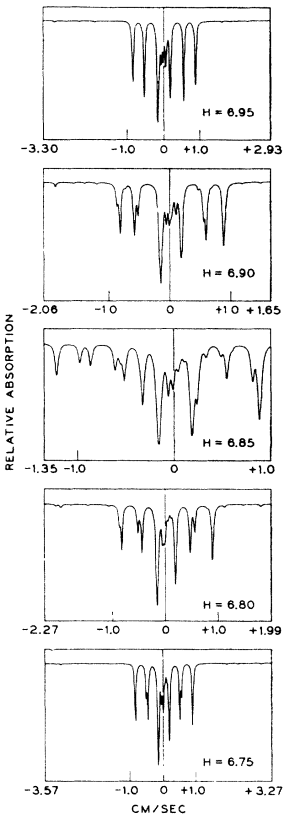

FIG. 7. Hyperfine spectra in the presence of mixing of states by the hyperfine interaction ($H\cong 6.9$ kOe). Markers are at ± 1.0 cm/sec.

the hyperfine interaction. As the field strength increases, the Zeeman term dominates the hyperfine interaction and the wave functions contain less and less admixtures of different $|M_S\rangle$ states. Finally, at $H=0.8$ kOe the spins are "polarized" in the field direction, M_S is a good quantum number, and the levels for the ground state, for example, are given by wave functions predominantly like $|M_S\rangle|m_I\rangle$ with energies $E(M_S+A(M_S m_I)$, $A\ll E$.

(2) $3.0\leq H\leq 4.0$ kOe. In this region a significant level repulsion occurs because of the small "a" term of the crystal field. At other values of field, this term is only of second-order importance, but in the region indicated it greatly affects the composition of the wave functions as noted above.

As long as the spacings of the electronic levels are large (>10 cm/sec), compared with the hyperfine interactions, ~1 cm/sec, the effective-field approximation is valid and each crystal-field level gives a hyperfine pattern of four lines with spacings determined by the field of $220\langle S_z\rangle$ with $\langle S_z\rangle$ in general different for each crystal-field level.

In this region $\langle S_z\rangle$ varies rapidly for the states ψ_2 and ψ_5. There are two prominent lines in Fig. 5 labeled M and I from ψ_2, and two lines from ψ_5 labeled E and T which are easily followed and illustrate the changing hyperfine fields. For $\psi_5(E,T)$ the hyperfine field of -550 kOe increases to a field of $+110$ kOe; E and T

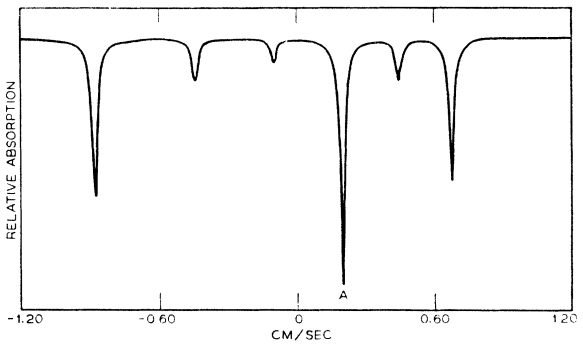

FIG. 8. Mössbauer pattern for the $|\pm\frac{1}{2}\rangle$ level.

move inward and this results in a decrease of the intensities of the two outermost lines. Simultaneously, the two inner lines M and I from ψ_2 move inward and then outward as H_{eff} from this level decreases from 110 kOe to 0 kOe and then to -550 kOe. Finally at about 4 kOe we see that the ordering *EMIT* has changed to *ITEM* and the transposition of pairs of lines is complete. Thus, the effect of small changes in the external field on certain crystal-field levels is to cause a reverasl of polarity of internal fields together with large changes in the internal fields which are orders of magnitude larger than the polarizing field.

(3) $4.2 \leq H \leq 4.4$ and $6.8 \leq H \leq 7.0$ kOe (Figs. 6 and 7). In the first of these regions, levels with $M_S = -\frac{3}{2}$ overlap with levels of $M_S = -\frac{1}{2}$ and in the second those with $M_S = -\frac{5}{2}$ with those of $M_S = -\frac{3}{2}$. A situation similar to that discussed in paragraph (1) occurs here. When their separation becomes comparable to the hyperfine interaction mixing again occurs via matrix elements such as $\langle M_S - 1, m_I + 1 | S_- I_+ | M_S, m_I \rangle$. In these cases, however, there is symmetrical behavior and by letting the program adjust the velocity scale to include all appreciable resonances independent of the Doppler energy it is seen that resonances at velocities out to ± 3 cm/sec can be expected. This is probably a fair estimate of the maximum separation of electronic levels that will allow this type of behavior and be consistent with the $\Delta M_S = 0$ selection rule we have assumed. Of course by relaxing this selection rule one could expect resonance out to velocities corresponding to the maximum separation of the electronic levels.

IV. DISCUSSION

The experimental data of Fig. 1 correspond to six values of $H_{\text{ext}} \leq 41$ kOe. With the background information of the previous section, it is now possible to discuss the spectra for each field value and compare theory and experiment.

(*a*) $H = 0$. The spectra from the middle doublet of composition $|\pm\rangle = |\pm\frac{3}{2}\rangle$ and the upper doublet, $|\pm\rangle = 0.9995|\pm\frac{5}{2}\rangle + 0.0327|\pm\frac{1}{2}\rangle$, are in agreement with the effective-field hfs expected from these levels.[1,2] In these levels $\langle + | S\pm | - \rangle$ vanishes so that hyperfine mixing does not occur and more importantly spin-spin relaxation of the type $|+\rangle \rightarrow |-\rangle$ does not occur since it is also a function of a similar matrix element. In the ground doublet, $|\pm\rangle = 0.9995|\pm\frac{1}{2}\rangle - 0.0327|\pm\frac{5}{2}\rangle$, the situation is quite different. Hyperfine mixing occurs and leads to the spectrum shown in Fig. 8. It is not entirely unexpected, however, that the corresponding spectrum cannot be extracted from the data. For one thing, spin relaxation can occur because $S_\pm$ now connects different electronic levels. Generally, the first effects of relaxation on a line are to broaden it and shift it towards the centroid of the spectrum.[9,10] Thus, the line marked A in Fig. 8 would tend to move toward zero velocity and broaden as a result of relaxation. In fact a pronounced line A' in Fig. 1, $H = 0$, appears near zero velocity and its presence might be explained in this manner. However, we found no other support for this reasoning and could not, for example, detect in the experimental data of Fig. 1 the other lines predicted by Fig. 8. Their absence conceivably could be connected with the fact that line A is the only line of the hfs spectra of the ground doublet that is *not* affected by off-diagonal elements of the hf tensor. Thus, small local fields, for example, from Al^{27} nuclei, exerting a few gauss on the Fe^{3+} iron would tend to wash out the other lines more rapidly than the transition A. Finally, this mechanism may compete with or complement the dipolar relaxation process discussed in previous work.[1,2] We noted above that fields ~ 10 Oe alter the spectrum due to this level when $\mathbf{H} \| z$. The g tensor from the ground doublet is $g_{\|} = 2$, $g_x = g_y = 6$. Thus fields of only 3 Oe in the x and y directions would be sufficient to perturb the "static hfs" which we have computed.

(*b*) *$H = 0.93$ kOe.* Reference to Fig. 2 shows that no levels are available which may mix via crystal-field or hyperfine terms. The electronic Zeeman term dominates the off-diagonal hyperfine terms, the spins are polarized, and the nuclei precess about the z direction; the effective-field approximation results. The theoretical and experimental spectra are in satisfactory agreement.

(*c*) *$H = 3.6$ kOe.* There are two main features of the data of Fig. 1: a significant decrease in intensity of the two outer lines and an increase in intensity and number of resonances in the middle $\sim\frac{3}{5}$ of the spectrum. It will be recalled that in this region the mixing via the small cubic term occurs. The effects of this mixing were given in Fig. 5 [hfs spectra $3.0 \leq H \leq 4.0$]. The decrease in intensity of the outer lines is explicable on the basis of the latter spectra since the hyperfine field from level 5 is now much smaller than 550 kOe. It is not possible to account quantitatively for the presence of the inner resonances because the field homogeneity severely limits the resolution of the complicated hfs patterns. This, of course, results from the rapid change in internal

[9] H. H. Wickman and A. M. Trozzollo, Phys. Rev. Letters **15**, 156 (1965).
[10] M. Blume, Phys. Rev. Letters **14**, 96 (1965).

fields as the external field varies over increments as small as 10–20 Oe. Since the variation of H_{ext} over the sample volume was ~180 Oe, we expect a distribution of spectra instead of a single well-resolved and easily interpreted spectrum. In spite of these difficulties, qualitative agreement between theory and experiment is still obtained. In particular the decrease in intensity of the outer lines is predicted and verified. Further, the distribution of inner resonances is consistent with a superposition of unresolved spectra.

(*d*) *H=11.0 kOe.* The situation here is analogous to that of (*b*) where mixing in negligible and the effective-field approximation holds.

(*e*) *H=27.5 kOe.* The change in the relative population of the $|-\frac{3}{2}\rangle$ and $|-\frac{5}{2}\rangle$ levels owing to the Boltzmann factor is apparent and the outer lines from the $|-\frac{5}{2}\rangle$ hfs levels now become more intense.

(*f*) *H=41.4 kOe.* The relative intensities of the spectra corresponding to different crystal-field levels are in agreement with Boltzmann factors.

V. CONCLUSIONS

We have discussed in detail some of the crystal-field effects and magnetic-field-dependent features of Mössbauer hfs in paramagnetic Fe^{3+}:Al_2O_3. The following points summarize the results:

1. Field strengths of the order of local fields in most paramagnetic systems are sufficient to destroy the static hfs from a level such as $|\pm\frac{1}{2}\rangle$ in iron. This can be extended to any doublet $|\pm\rangle$ which has significant nonvanishing matrix elements of the dipole operators $S_\pm$:$\langle+|S_+|-\rangle$, etc.

2. Depending on the external field strength a considerable mixing of states by the hyperfine interaction can occur and result in complex Mössbauer spectra. This, of course, has implications for Mössbauer experiments with polycrystalline absorbers where such effects can be present over considerable field ranges due to the random orientation of individual ions.

3. Mixing by small terms in the crystal-field spin Hamiltonian produces interesting and rather simple changes in internal hyperfine fields. If such behavior is found in the ground electronic level of an ion it could be used as a broad-band method of adjusting internal fields and even selecting their polarity. An obvious and useful extension of these ideas is to the case of certain rare-earth Mössbauer systems, in particular Eu^{2+}, another S state ion with small zero-field splittings.

APPENDIX

Recall that 24 and 12 energy levels are associated with the complete hyperfine spin Hamiltonians $\mathcal{H}_e$ and $\mathcal{H}_g$, respectively. Thus, for the ith ground-state level, we have

$$\Psi_i=\sum_{M_S,m_I} a_i(M_S,m_I)\left|\tfrac{5}{2},M_S\right\rangle\left|\tfrac{1}{2},m_I\right\rangle, \qquad \text{(A1)}$$

and for the excited state

$$\varphi_j=\sum_{M_S,m_I} b_j(M_S,m_I)\left|\tfrac{5}{2},M_S\right\rangle\left|\tfrac{3}{2},m_I\right\rangle. \qquad \text{(A2)}$$

The relative intensity of radiation absorbed from a γ-ray beam at an angle θ relative to the direction of the quantization axes in (A1) and (A2) may be written in simplified form as

$$I_{ij}(\theta)=2(\sin^2\theta)|\langle\Psi_i|T_0^1|\varphi_j\rangle|^2+(1+\cos^2\theta)\times[|\langle\Psi_i|T^1_{-1}|\varphi_j\rangle|^2+|\langle\Psi_i T^1_{+1}|\varphi_j\rangle|^2], \qquad \text{(A3)}$$

where T_q^1 are the components of a first-rank tensor describing the $M1$ radiation. The wave functions of Eqs. (A1) and (A2) may be substituted in (A3) and the intensities obtained as a function of the coefficients a_i and b_j. This was carried out by a computer program. Finally, the line positions in Doppler energy (cm/sec) may be simply written

$$E_{ij}=W+E_j-E_i,$$

where W represents the isomer shift and may be conveniently set equal to zero. The final spectra where obtained by placing a Lorentz curve (or half-width 0.04 cm/sec) with intensity $I_{ij}(\theta=0)$ at E_{ij}; the total spectrum was a superposition of the various components, 288 in all, many of which had vanishing intensity due to the selection rules of the first-rank tensor T_q^1.